Purdue University
Purdue e-Pubs

International Refrigeration and Air Conditioning Conference

School of Mechanical Engineering

2016

Characterization of nanofluids formed by fumed Al2O3 in water for geothermal applications

Sergio Bobbo
Istituto per le Tecnologie della Costruzione – Consiglio Nazionale delle Ricerche, Italy, sergio.bobbo@itc.cnr.it

Laura Colla
Istituto per le Tecnologie della Costruzione – Consiglio Nazionale delle Ricerche, Italy, laura.colla@itc.cnr.it

Antonella Barizza
Istituto per le Tecnologie della Costruzione – Consiglio Nazionale delle Ricerche, Italy, antonella.barizza@itc.cnr.it

Stefano Rossi
Istituto per le Tecnologie della Costruzione – Consiglio Nazionale delle Ricerche, Italy, stefano.rossi@itc.cnr.it

Laura Fedele
Istituto per le Tecnologie della Costruzione – Consiglio Nazionale delle Ricerche, Italy, laura.fedele@itc.cnr.it

Follow this and additional works at: http://docs.lib.purdue.edu/iracc

Characterization of nanofluids formed by fumed Al_2O_3 in water for geothermal applications

Sergio BOBBO[1], Laura COLLA[1], Antonella BARIZZA[1], Stefano ROSSI[1], Laura FEDELE[1,*]

[1]Istituto per le Tecnologie della Costruzione – Consiglio Nazionale delle Ricerche
Corso Stati Uniti, 4
45127 Padova
Email: laura.fedele@itc.cnr.it

* Corresponding Author

ABSTRACT

The European Project Cheap-GSHPs, recently approved, aims at reducing the total cost of shallow geothermal systems by 20-30%, also improving actual drilling/installation technologies and designs of Ground Source Heat Exchangers (GSHEs), in combination with a holistic engineering approach to optimize the entire systems for building and district heating and cooling applications, across the different underground and climate conditions existing within the EU. In this frame, the efficiency of the system heat pump/GSHE will be an important task and a part of this project will be on the analyses of possible alternative secondary fluids to be used in the geothermal probe. Here, two different commercial suspensions of fumed Al_2O_3 nanoparticles in water will be considered as possible efficient secondary fluid. Four different concentrations will be studied for each nanofluid, *i.e.* 3%, 5%, and 30% or 40%, and the stability, thermal conductivity and dynamic viscosity of these fluids will be characterized, in order to analyse their possible employment as thermal fluids.

1. INTRODUCTION

Nanofluids, *i.e.* suspensions of nanometric solid particles (metal oxides, metals, carbon, etc.) in liquids (such as, for example, water, glycols, oils and coolants), have been proposed, due to their thermal, rheological and tribological properties, as promising fluids for various applications [*e.g.* Choi (2009), Saidur *et al*. (2011), Celen *et al*. (2014), Yu *et al*. (2007)].

In particular, in the geothermal field, some nanofluids have been proposed as possible thermal vectors, promising high heat transfer efficiency and better performance.

Recently, a project, called "Improving the Efficiency of Geothermal Heat Pumps", has been founded by the U.S. Environmental Protection Agency's Small Business Innovation Research Program (KIT, 2012). In this project, the employment of nanofluids formed by fumed alumina (Al_2O_3) dispersed in water or water and propylene glycol mixtures was found to improve the heat transfer and the overall efficiency of the geothermal heat pumps (GHPs) systems (Patent US, 2011). For this reason, in order to evaluate a possible operating fluid for the systems studied in the European Project Cheap-GSHPs, two commercial suspensions of fumed Al_2O_3 in water were studied at different compositions.

Stability and thermal conductivity of these nanofluids have been carefully characterized and will be described in this paper. Also dynamic viscosity was analysed in order to evaluate the nanofluids performance as geothermal fluid. At this scope, Mouromtseff numbers were considered to estimate the thermal effectiveness of the these nanofluids compared with water.

2. EXPERIMENTAL

2.1 Materials
Two different commercial nanofluids, produced by Evonik, were used in this study: Aerodisp W440 and Aerodisp W630. Both are water based nanofluids with Al_2O_3 at 40 wt% and 30 wt%, respectively. Negligible amounts of bio-

cides and preservatives are dispersed in the nanofluids. No information are available about the presence of dispersants.

Bidistilled water (CARLO ERBA, Bidistilled water, CAS Nr 7732-18-5) was used to dilute the original nanofluid and obtain other nanofluid compositions (0.5 wt%, 3 wt% and 5 wt%). After sonicating the original nanofluids for 1 h, the amount of bidistilled water necessary to obtain the various compositions was weighed by an analytical balance (Gibertini E42S 240 g FS), with an uncertainty of 0.002 g, and added to sample of the original nanofluids.

### 2.2 Nanofluid preparation and stability characterization

A Zetasizer Nano ZS (Malvern), based on the Dynamic Light Scattering (DLS), was used to analyse the average dimension of the nanoparticles in solution. A detailed description of this apparatus has been given in previous paper (Fedele *et al*., 2012). The range of size which can be measured is from 0.6 nm to 6 μm. All size measurements were taken at 298 K. To perform optimal size measurements, samples of the original nanofluids were diluted to 0.5%, considering dimensional distribution of nanoparticles inside the solution is generally independent on the concentration [*e.g*. Colla *et al*. (2014)].

After sonication, the Al_2O_3 mean particle diameter, measured 3 times for each sample, was around 136 nm for W440 and 149 nm for W630: Fig. 1 shows the particle size distribution, according to the intensity detected by the Zetasizer. The absence of particle micrometer-sized aggregates confirmed the good stability of the obtained dispersions. The following analysis was made to determine the tendency of the particles in suspension to settle down along time. Two samples of the fluid were put in two different measurement cuvettes. The first sample was measured almost every day for thirty-one days, without shaking the fluid, to evaluate the changes in size distribution due to natural sedimentation. The second sample was also measured almost every day for thirty days after sonication of the fluid to evaluate the changes in size distribution after mechanically removing the sedimentation. The variation along time of Al_2O_3 nanoparticle mean diameters are shown in Fig. 2. In the case of static solutions, the mean size
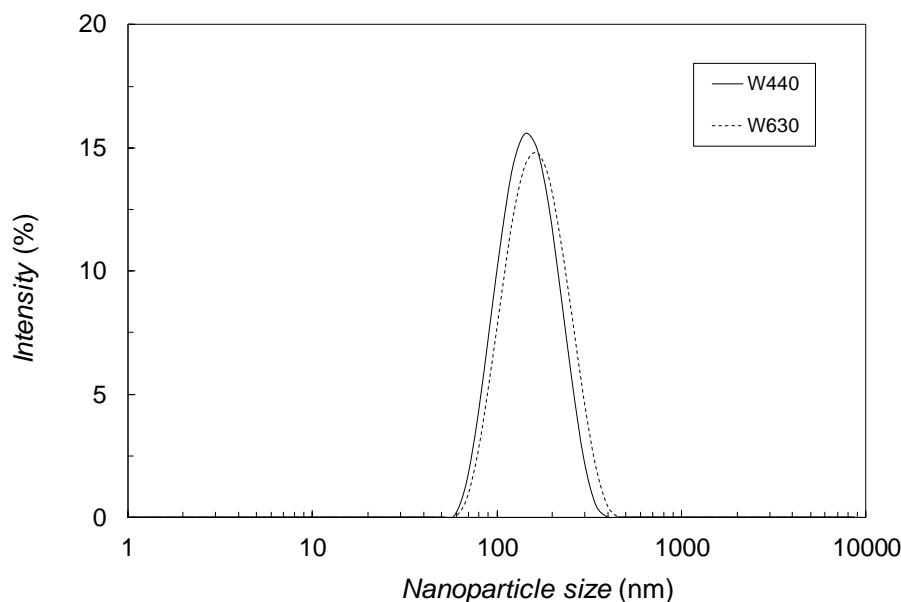
Figure 1: Nanoparticle size distribution for the W440 and W630 nanofluids diluted at 0.5 wt%

slightly decreased to around 82 nm for W440 and to 95 nm after 31 days, indicating a partial precipitation. However, after sonication for 1 h (second sample), a mean particle size very close to the original was always recorded for both fluids, suggesting the absence of further aggregation phenomena. This behavior suggests the fluids could be applied in systems were the forced circulation allows to continuously stir them, preventing the deposition of nanoparticles and maintaining the size distribution as in the original fluids.
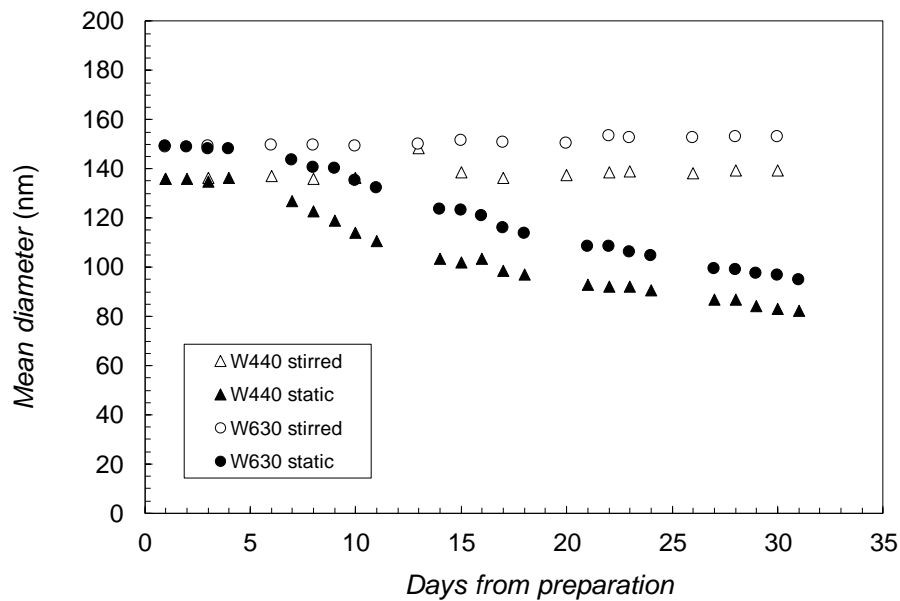
Figure 2: The variation along time of the nanoparticle mean diameters. Empty symbols stay for stirred samples,

The Zeta potential of nanoparticles was measured by the Zetasizer Nano (Malvern). In general, the higher the Zeta potential, the higher the stability of the particles in suspension. Al_2O_3–water nanofluid Z potential was around 49.6 mV for W630 and 47.5 mV for W440, both higher than the empirical limit of 30 mV over which a colloidal solution should be stable.

2.3 Dynamic Viscosity
Some preliminary viscosity measurements have been performed in the temperature range between 303 K and 323 K at atmospheric pressure for the suspensions W440 at 40 wt% and W630 at 30%, and also for the diluted W440 at 3 wt% and 5 wt%, by means of a rotational rheometer with a plate-cone geometry (AR-G2 rheometer TA Instruments), applying the methodology described in Bobbo *et al*. (2012). The declared instrument accuracy is 5%, even if the tests performed on water showed an uncertainty lower than 2% (as explained below in 3.1).

2.4 Thermal Conductivity
Thermal conductivity data were measured at ambient pressure and in a temperature range between 283 K and 323 K by means of a TPS 2500 S (Hot Disk), shown in Fig. 3. It is based on the hot disk technique and can measure the thermal conductivity and thermal diffusivity of several materials. A description of the apparatus is given in Fedele *et al*. (2012), while a theoretical description of this method is provided in He (2005). In case of liquids, the sensor is immersed in the fluid and a full contact is provided by means of a specifically built container, maintained at isothermal condition by a water thermostatic bath. The power supplied for each measurement was 40 mW and the
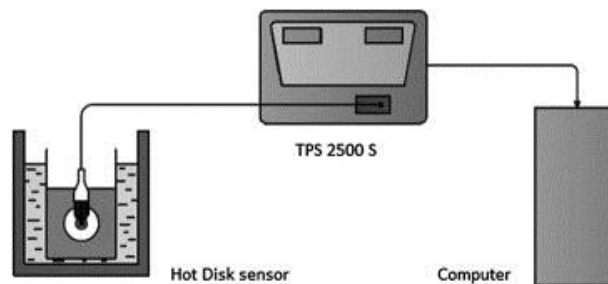
Figure 3: Scheme of the thermal conductivity measurements apparatus (TPS 2500 S, hot disk).

time of the power input was 4 s. The declared instrument accuracy is 5%, even if the tests performed on water showed an uncertainty around 1% (as explained below in 3.1).

3. RESULTS AND DISCUSSION

3.1 Experimental results

3.1.1 Dynamic viscosity: Viscosity data are necessary to understand the actual potentiality of the fluids to be employed as thermal vectors in the geothermal probe. Some preliminary tests were performed in order to identify the best fluids for this application.

To test the actual accuracy of the rheometer, water dynamic viscosity was measured in the temperature range between 303 K and 323 K. The results were compared with Refprop 9.1 database (Lemmon *et al.*, 2010), and the data agreed well within 2%.

Some viscosity measurements were initially performed for the original solutions W440 and W330, at 40 wt% and 30 wt%, respectively. The results, shown in Table 1, taken at atmospheric pressure and 313 K and 323 K, indicate a huge viscosity enhancement, due to the high nanoparticles concentrations, especially for the W630. In fact, even if the concentration is lower (30 wt% instead of 40 wt%) for this nanofluid, the viscosity increases more than 100 times that of water.

This difference is probably due to the presence of different dispersants in the suspensions. For this reason, the solution W630 was disregarded and the attention moved on the W440, trying to find the optimal compromise between the enhancement in thermal conductivity and dynamic viscosity with the proper dilution.

Then, the solution W440, at 40 wt%, was diluted at 3 wt% and 5 wt%. Preliminary results show an enhancement in terms of dynamic viscosity up to 5% for the solution at 3 wt% and up to 20% for the solution at 5 wt%, both at 303 K and 323 K. However, more experimental data are needed to better understand the rheological behaviour of these fluids.

Table 1: Dynamic viscosity and dynamic viscosity enhancement related to pure water (from Refprop 9.1 database) as a function of temperature

W440 40 wt%			W630 30 wt%		
T (K)	μ (Pa·s)	μ_{xp}/μ_{water}	T (K)	μ (Pa·s)	μ_{exp}/μ_{water}
313	0,01130	17,3	313	0,06717	102,9
323	0,00965	17,6	323	0,07656	140,0
W440 3 wt%			W440 5 wt%		
T (K)	μ (Pa·s)	μ_{xp}/μ_{water}	T (K)	μ (Pa·s)	μ_{exp}/μ_{water}
303	0,000839	1,05	303	0,000915	1,15
323	0,000571	1,04	323	0,000656	1,20

3.1.2 Thermal conductivity: Thermal conductivity of the selected nanofluids was measured with the aim to evaluate the enhancement on the thermal conductivity of water, as a function of concentration and temperature, obtained by adding Al_2O_3 nanoparticles.

To estimate the actual accuracy of the measurements, tests have been performed with water in the given range of temperatures. By comparison with thermal conductivity data calculated with Refprop 9.1 database (Lemmon *et al.*, 2010), the experimental data differed from literature less than 1%, well within the 5% uncertainty declared by the manufacturer.

Table 2 reports the data obtained from the measurements for all the nanofluids in the range of temperatures between 283.15 K and 333.15 K. Fig. 4 represents the thermal conductivity as a function of temperature. Thermal conductivity of nanofluids was higher than that of water and basically increased with temperature for all the nanofluids. At the same time, thermal conductivity clearly increased with reference to water at increasing

nanoparticles concentration. The fluctuation in experimental results are mainly related to the uncertainties in the measurements.

Table 2: Thermal conductivity and thermal conductivity enhancement related to pure water from Refprop 9.1 database as a function of temperature

W440 3 wt%			W440 5 wt%			W440 40 wt%		
T (K)	λ (W/m K)	$\lambda_{exp}/\lambda_{water}$	T (K)	λ (W/m K)	$\lambda_{exp}/\lambda_{water}$	T (K)	λ (W/m K)	$\lambda_{exp}/\lambda_{water}$
284.3	0.604	1.04	283.9	0.611	1.05	284.1	0.798	1.37
293.2	0.609	1.02	293.7	0.618	1.03	293.5	0.801	1.34
303.3	0.639	1.04	303.6	0.645	1.05	303.6	0.833	1.35
313.6	0.666	1.06	313.5	0.672	1.07	313.4	0.855	1.36
323.3	0.695	1.09	323.3	0.699	1.09	323.3	0.881	1.37
333.6	0.706	1.08	333.6	0.718	1.10	333.3	0.884	1.35

W630 30 wt%		
T (K)	λ (W/m K)	$\lambda_{exp}/\lambda_{water}$
283.9	0.700	1.20
293.8	0.710	1.18
305.9	0.732	1.18
313.3	0.754	1.20
323.3	0.766	1.19
333.2	0.778	1.19
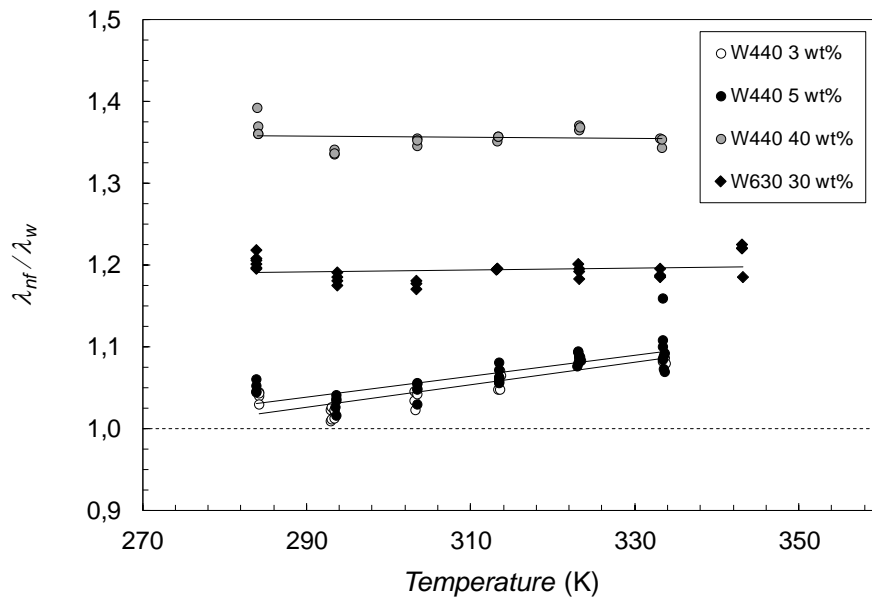
Figure 5: Thermal conductivity enhancement as a function of temperature (interpolation lines highlight the trends only)

Figure 5 reports the enhancement expressed as the ratio between the thermal conductivity of the nanofluids and that of water, calculated with Lemmon *et al.* (2010). At the lower concentrations, the enhancement is quite low at lower temperatures. However, it increases and becomes significant at the higher temperatures, being more than proportional with respect to concentration (up to 10% for W440 5 wt%). This is connected to the almost linear dependence of thermal conductivity of nanofluids with temperature, while water thermal conductivity increases less when temperature increases. The enhancement for the nanofluids at higher concentrations is practically constant with temperature and less than proportional with respect to the concentration (around 36% for W440 40 wt% and around 20% for W630 30 wt%).
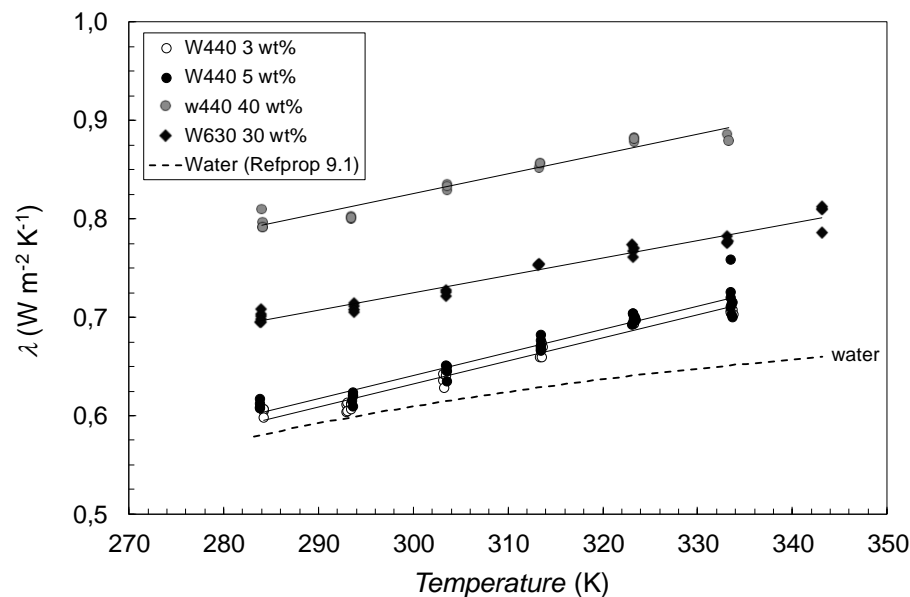
Figure 4: Thermal conductivity as a function of temperature (interpolation lines highlight the trends only)

, Page 7

3.2 Mouromtseff number

A theoretical evaluation of the heat transfer behaviour of a fluid can be performed by calculating the Mouromtseff number applying the general expression, valid for single phase forced convection (Mouromtseff, 1942)

$$Mo = \frac{\lambda^a \rho^b c_p^c}{\mu^d} \qquad (1)$$

For a fluid flowing in a fixed geometry at given velocity, the larger the Mouromtseff number the larger will be the heat transfer rate. To apply this equation, valid at given temperature, it is then necessary to know the properties involved: thermal conductivity, density, heat capacity and dynamic viscosity. In the case of nanofluids, thermal conductivity and viscosity must be measured being not linearly dependent on nanoparticles concentration, while density and heat capacity can be calculated assuming a linear behaviour with reference to volumetric fraction applying the following equations:

$$\rho_{nf} = \phi \cdot \rho_{np} + (1 - \phi) \cdot \rho_{bf} \qquad (2)$$
$$\rho_{nf} \cdot c_{p_{nf}} = \phi \cdot \rho_{np} \cdot c_{p_{np}} + (1 - \phi) \cdot \rho_{bf} \cdot c_{p_{bf}} \qquad (3)$$

The enhancement in heat transfer obtainable adding nanoparticles to water can be evaluated through the ratio between the *Mo* number for the nanofluid and that of water. If the ratio is higher than 1, the nanofluid is more efficient in heat transfer than water.

In this case, the Mouromtseff number can be calculated for W440 3 wt% and W440 5 wt% at 303 K and 323 K.

In case of internal laminar regime, the ratio is given simply by:

$$\frac{Mo_{nf}}{Mo_w} = \frac{\lambda_{nf}}{\lambda_w} \qquad (4)$$

In case of internal turbulent flow, the Mo number is given by the following expression:

$$Mo = \frac{\lambda^{0.67} \rho^{0.8} c_p^{0.88}}{\mu^{0.47}} \qquad (5)$$

and then the ratio is obtained by applying this equation to the nanofluid and the water.

By applying equations 1 to 5, the following values, summarized in Table 3, for the ratio of Mouromtseff number has been achieved for laminar and turbulent flow regime at the temperatures 303 K and 323 K.

Table 3: Relative heat transfer through Mouromtseff number between nanofluid W440 3 and 5 wt% and water at 303 K and 323 K in laminar flow regime and turbulent flow regime.

T (K)	Mo_{nf}/Mo_w			
	W440 3 wt%		W440 5 wt%	
	Laminar flow	Turbulent flow	Laminar flow	Turbulent flow
303	1.04	1.01	1,05	0,99
323	1.08	1.05	1,09	0,99

The enhancement is higher in laminar flow than in turbulent flow for both fluids, as already observed in other cases (e.g. Bobbo *et al.*, 2011). In laminar flow, the enhancement is similar for the two fluids, and increasing with temperature from around 5% at 303 K to around 9% at 323 K. In turbulent flow, only W440 3 wt% shows some increment, even if relatively significant only at 323 K (around 5%). W440 5 wt% is penalised by the higher viscosity at both the considered temperatures. These results, even if only theoretical and preliminary, being connected to limited experimental results, suggest the possibility that the at least W440 3 wt% could be successfully applied in the geothermal especially at the higher temperatures.

4. CONCLUSIONS

Under the European Project "Cheap and efficient application of reliable Ground Source Heat exchangers and Pumps" Cheap-GSHPs, recently approved, with the ambition to reduce the total cost of shallow geothermal systems by 20-30%, several nanofluids will be tested as possible secondary fluids in the heat pump-geothermal probe system.

Two different commercial suspensions of fumed Al_2O_3 nanoparticles in water were considered in this work and the less penalising in terms of lower viscosity was considered for additional dilution, in order to get the best compromise between thermal conductivity and dynamic viscosity. Stability, thermal conductivity and dynamic viscosity were analysed for four different concentrations, *i.e*. 3%, 5%, and 30% or 40%.

According to the results and a preliminary analysis of the Mouromtseff number, the fluid with the lowest concentration, *i.e.* W440 3 wt%, seems to have some possibility to be applied, at least at temperatures higher than 40-50°C. With reference to the heat pump system under development within the project, this means the nanofluid will be probably not suitable as thermal vector in the ground loop, while it could be used as a secondary fluid to distribute heat from the condenser either to fan coils (inlet temperatures around 40-50°C) or to radiators or air heaters (inlet temperatures around 60-70°C). However, additional measurements, in particular viscosity and heat transfer coefficient, are necessary and will be performed in the near future to better understand its applicability and potentiality in the final system.

NOMENCLATURE

c_p	specific heat	(J/kg K)
Mo	Mouromtseff number	(-)
T	temperature	(K)
wt%	nanoparticles weight fraction	(%)

Greek symbols

λ	thermal conductivity	(W/m K)
ρ	density	(kg/m^3)
μ	dynamic viscosity	(Pa s)
ϕ	nanoparticles volumetric fraction	(-)

Subscript

exp	experimental
nf	nanofluid
np	nanoparticles
w	water

ACKNOWLEDGEMENT

REFERENCES

Acta Technology. Website http://acta-technology.com/products-_acta.html#GSHP

Bobbo, S., Fedele, L., Benetti, A., Colla, L., Fabrizio, M., Pagura, C., Barison, S. (2012). Viscosity of water based SWCNH and TiO_2 nanofluids, *Exp. Therm. Fluid Sci*., 36, 65–71.

Bobbo, S., Colla, L., Scattolini, M., Agresti, F., Barison, S., Pagura, C., Fedele, L. (2011). Thermal conductivity and viscosity measurements of water-based silica nanofluids, Proceedings of the 2011 NSTI Nanotechnology Conference and Expo, Boston, USA, pp. 478-481 –205.

Celen,A. Çebi, M. Aktas, O. Mahian, A. S. Dalkilic & S. Wongwises (2014). A review of nanorefrigerants: Flow characteristics and applications, *Int. J. Refrig., 44*, 125-140.

Choi, S. U. S. (2009). Nanofluids: From Vision to Reality Through Research, *J. Heat Transf., 131*.

Colla, L., Marinelli, L., Fedele, L., Bobbo, S. & Manca, O. (2014). Characterization and simulation of the heat transfer behaviour of water-based ZnO nanofluids, *J. Nanosci. Nanotechno., 14*, 1-11.

Fedele, L., Colla, L. & Bobbo, S. (2012). Viscosity and thermal conductivity measurements of water-based nanofluids containing titanium oxide nanoparticles, *Int. J. Refrig., 35*, 1359-1366.

He, Y. (2005). The rapid thermal conductivity measurement with a hot disk sensor Part 1. Theoretical considerations, *Thermochim. Acta, 436*, 122-129.

KIT - KEILIR INSTITUTE OF TECHNOLOGY (2012). Improving the Efficiency of Geothermal Heat Pumps, website http://www.keilir.net/technology/technology/news/improving-the-efficiency-of-geothermal-heat-pumps

Lemmon, E. W., Huber, M. L., McLinden, M. O. (2010). NIST Standard Reference Database 23, Reference Fluid Thermodynamic and Transport Properties (REFPROP), version 9.1; National Institute of Standards and Technology: Gaithersburg, MD.

Mouromtseff, I. E. (1942). Water and Forced-Air Cooling of Vacuum Tubes Nonelectronic Problems in Electronic Tubes, Proceedings of the Institute of Electrical and Electronics Engineers (IEEE), New Yersey, USA, pp. 190–205

Patent US 8580138 B2, Nanofluids and a method of making nanofluids for ground source heat pumps and other applications, US 13/229,737, registered 11/09/2011, inventor John Melvin Olson, Acta Technology Inc

Saidur, K.Y. Leong & H.A. Mohammad (2011). A review on applications and challenges of nanofluids, *Renew. Sust. Energ. Rev., 15*(3), 1646–1668.

Yu, W., France, D.M., Choi, S.U.S. & Routbort, J.L. (2007). Review and Assessment of Nanofluid Technology for Transportation and Other Applications, Report, Argonne Laboratory.